Comprehensive approach to coregistration of autoradiography and microscopy images acquired from a set of sequential tissue sections

Introduction: The exploration of tumor microenvironment has been translated to diagnostic imaging through the field of molecular imaging. Specific biomarker probes can be administered and visualized in vivo with the aid of functional imaging modalities such as positron emission tomography (PET). Furthermore, it has been suggested that by creating and delivering heterogeneous dose distributions based on PET imaging, the efficiency of radiation treatment may be increased considerably[1, 2]. Phase I dose escalation trials based on ^{18}F-FDG imaging have been already conducted[3, 4]. In validating PET tracers intended for guidance of highly conformal treatments such as intensity modulated radiotherapy, one of the initial steps should be to establish if the intratumoral uptake of the tracer is spatially concordant with its biological target. By performing statistical analysis of the uptake patterns observed on digital autoradiography images (DAR) and the distribution of biological markers on microscopy images obtained from the same tumor sections, one could potentially reveal if the PET tracer is specifically binding to its intended target. However, before ascribing any level of confidence to observed spatial concordance or lack thereof, it is necessary to make sure that the images are properly coregistered.

The study presented here had two objectives: to propose a comprehensive a protocol for coregistration of DAR and microscopy images obtained from thin sections of xenograft tumors, and to evaluate its accuracy. This study was specifically aimed at creating a tool for ^{18}F-FLT validation as a marker of cell proliferation, but this methodology can be applied to any other PET tracer validation or any compound that could be labeled with a positron emitter.

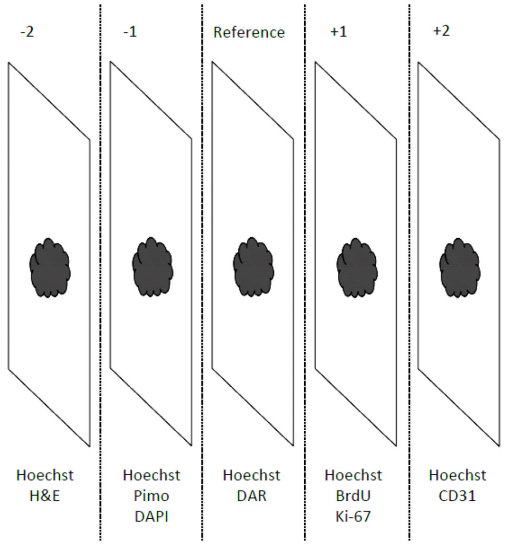

Figure 1. Sketch of systematic assignment of image acquisition modality to relative position of the tissue sample in each sequential stack. Reference sections were always assigned to DAR acquisition. Hoechst (blood flow surrogate), H&E (tissue viability), Pimo (hypoxia), DAPI (cell nuclei), BrdU and Ki67 (cell proliferation), CD31 (vasculature).

Methods: Human head and neck tumor xenografts were developed in athymic mice. The employed methodology for developing the animal tumors and obtaining the DAR and microscopy images was described earlier[5]. Sequential stacks of tumor sections were obtained from each tumor. From each of these stacks, one section (reference) was utilized for DAR imaging, to obtain the FLT microscopic distribution. On these **reference** sections, registration landmarks were manually placed around the tissue section. Unfortunately, all necessary microenvironmental information for FLT histopathological validation could not be retrieved from this single section. Therefore, adjacent sections were utilized for microscopy imaging in order to reveal multiple functional aspects of the tumor (Figure 1). 8µm tumor sections were obtained, a section thickness that is considerably smaller than the typical feature size of tumor microenvironment, as revealed by microscopy (about 100µm). Assuming tumor microenvironment contiguity throughout the sequential stack, adjacent sections were characterized by the same patterns of microenvironmental features, even if cell-to-cell correspondence was not implied. The non-reference sections were automatically processed for microscopy.

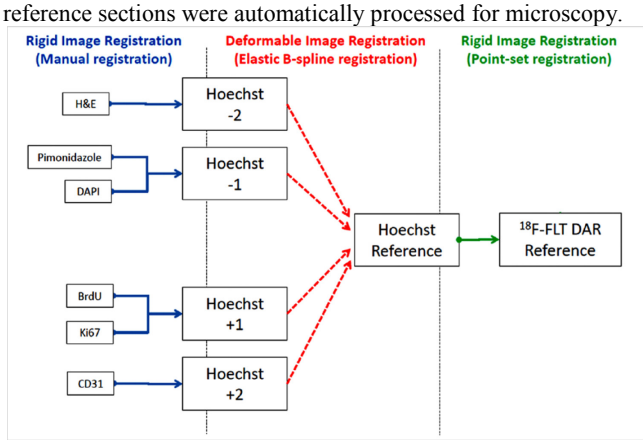

Figure 2. Registration scheme utilized for each sequential image set.

The end-goal of the method proposed here is objective coregistration of DAR and microscopy images acquired from several sequential sections. In order to accomplish that, we used a multi-step approach (Figure 2). First, for each tumor tissue section used, all images obtained from that particular sections were rigidly registered, since each tissue sample was rigidly fixed onto the glass slide between obtaining the different images. Hoechst to DAR image registration was accomplished by rigid point set registration based on the external landmarks visible around the tumor section on both imaging modalities. Thereafter, these independent sets of rigidly registered images were registered together using deformable registration. Inherent to the tissue cutting and slide preparation process is the presence of numerous non-linear deformations (tissue stretching, warping, etc.), which were previously mentioned in histopathological image registration studies[6, 7]. As each tissue section had its own characteristic deformations, deformable image registration was needed to correctly align images that were obtained from different sections. As represented schematically in Figure 1, **Hoechst images were obtained from all tumor sections**. Utilizing the biological correspondence established by the microenvironmental contiguity between adjacent tissue sections, the non-reference Hoechst images were deformably registered to the reference Hoechst image utilizing the plugin bundle called Fiji (implemented in the NIH ImageJ platform). The final transformations for each non-reference Hoechst image were applied to all other microscopy images obtained from the same tissue section (Figure 3). At this point all obtained images were registered to the ^{18}F-FLT DAR, and had a resolution of 2.5µm/pixel.

In order to assess the accuracy of the registration procedure, sets of corresponding landmarks were defined on each image, independent of those utilized for registration. The average displacement of corresponding points after registration was defined as the

registration error in both cases. The total registration error was defined as the convolution of the two error components (rigid and deformable) represented as Gaussian distributions.

Results: The estimated error in the rigid registration was 30.8µm±20.1µm for Hoechst to ^{18}F-FLT DAR image registration. The error in manual alignment of microscopy images coming from the same tumor section was considered negligible. The estimated error in the deformable registration was 23.1µm±17.9µm. Based on these observations, the computed total error reached 44.86µm.

Discussion: The registration error reported here is smaller than estimated values previously estimated between 100-200µm[5, 8, 9]. This significant lowering in registration error enables more accurate spatial correlation studies between PET tracer intratumoral distributions and that of different microenvironmental factors, as it represents less than two pixels error on original resolution of the DAR. While this study presented the coregistration procedure utilizing animal tumors, the methodology can be readily translated to human specimens, for PET histopathological validation at clinical level.

Conclusion: In conclusion, we have introduced a comprehensive, semi-automated method of coregistering DAR and microscopy images based on corresponding Hoechst immunofluorescent microscopy images. The registration procedure addresses the significant non-linear deformations induced by tissue processing, and eliminates the need for manual alignment of images from adjacent sections, or image content-based registration. Increased statistical significance of spatial concordance analysis between PET tracer uptake and relevant tumor markers, translates in more confident interpretation of PET images at the clinical level, and more biologically pertinent assignment of dose for future dose escalation studies based on functional imaging data.

1. Ling CC, Humm J, Larson S, et al. Towards multidimensional radiotherapy (MD-CRT): Biological imaging and biological conformality. *Int J Radiat Oncol Biol Phys*. 2000;47:551-560.
2. Toma-Daşu I, Daşu A, Brahme A. Dose prescription and optimisation based on tumour hypoxia. *Acta Oncol*. 2009;48:1181-1192.
3. Duprez F, De Neve W, De Gersem W, Coghe M, Madani I. Adaptive dose painting by numbers for head-and-neck cancer. *Int J Radiat Oncol Biol Phys*. 2010.
4. Madani I, Duthoy W, Derie C, et al. Positron emission tomography-guided, focal-dose escalation using intensity-modulated radiotherapy for head and neck cancer. *Int J Radiat Oncol Biol Phys*. 2007;68:126-135.
5. Pugachev A, Ruan S, Carlin S, et al. Dependence of FDG uptake on tumor microenvironment. *Int J Radiat Oncol Biol Phys*. 2005;62:545-553.
6. Schormann T, Dabringhaus A, Zilles K. Statistics of deformations in histology and application to improved alignment with MRI. *IEEE Trans Med Imaging*. 1995;14:25-35.
7. Arganda-Carreras I, Sorzano COS, Thvenaz P, et al. Non-rigid consistent registration of 2D image sequences. *Phys Med Biol*. 2010;55:6215-6242.
8. Busk M, Horsman M, Jakobsen S, et al. Imaging hypoxia in xenografted and murine tumors with 18F-fluoroazomycin arabinoside: A comparative study involving microPET, autoradiography, PO2-polarography, and fluorescence microscopy. *Int J Radiat Oncol Biol Phys*. 2008;70:1202-1212.
9. Hoeben BAW, Kaanders JHAM, Franssen G, et al. PET of hypoxia with 89Zr-labeled cG250-F(ab')2 in head and neck tumors. *The Journal of Nuclear Medicine*. 2010;51:1076-1083.

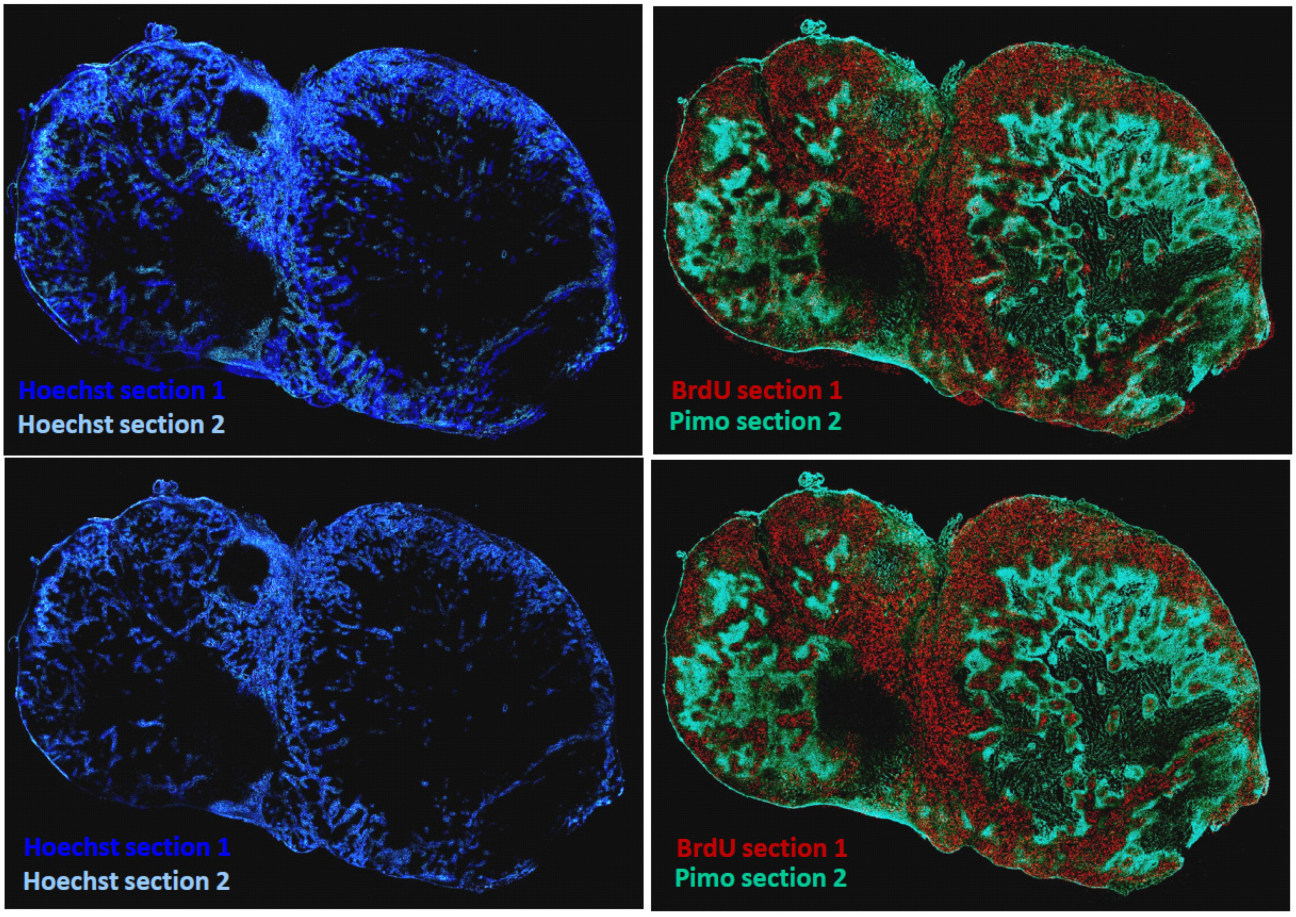

Figure 3. Transparent image overlay presenting deformable image registration results. Top row presents microscopy images rigidly registered only. Bottom row presents images after deformable registration. The transformations were calculated based on Hoechst image registration, and applied to the other microscopy images.